0026-895X/08/7404-1141–1151$20.00
MOLECULAR PHARMACOLOGY
Vol. 74, No. 4
49064/3387926
Mol Pharmacol 74:1141–1151, 2008
Printed in U.S.A.

Selective Inhibition of Mitogen-Activated Protein Kinase Phosphatases by Zinc Accounts for Extracellular Signal-Regulated Kinase 1/2-Dependent Oxidative Neuronal Cell Death

Yeung Ho, Ranmal Samarasinghe, Megan E. Knoch, Marcia Lewis, Elias Aizenman, and Donald B. DeFranco

Department of Neuroscience, University of Pittsburgh, Pittsburgh, Pennsylvania (Y.H., R.S.); and Departments of Neurobiology (M.E.K., E.A.) and Pharmacology and Pittsburgh Institute for Neurodegenerative Diseases (M.L., D.B.D.), University of Pittsburgh School of Medicine, Pittsburgh, Pennsylvania

Received May 21, 2008; accepted July 16, 2008

ABSTRACT

Oxidative stress induced by glutathione depletion in the mouse HT22 neuroblastoma cell line and embryonic rat immature cortical neurons causes a delayed, sustained activation of extracellular signal-regulated kinase (ERK) 1/2, which is required for cell death. This sustained activation of ERK1/2 is mediated primarily by a selective inhibition of distinct ERK1/2-directed phosphatases either by enhanced degradation (i.e., for mitogen-activated protein kinase phosphatase-1) or as shown here by reductions in enzymatic activity (i.e., for protein phosphatase type 2A). The inhibition of ERK1/2 phosphatases in HT22 cells and immature neurons subjected to glutathione depletion results from oxidative stress because phosphatase activity is restored in cells treated with the antioxidant butylated hydroxyanisole. This leads to reduced ERK1/2 activation and neuroprotection. Furthermore, an increase in free intracellular zinc that accompanies glutathione-induced oxidative stress in HT22 cells and immature neurons contributes to selective inhibition of ERK1/2 phosphatase activity and cell death. Finally, ERK1/2 also functions to maintain elevated levels of zinc. Thus, the elevation of intracellular zinc within neurons subjected to oxidative stress can trigger a robust positive feedback loop operating through activated ERK1/2 that rapidly sets into motion a zinc-dependent pathway of cell death.

Oxidative stress results from the accumulation of reactive oxygen species (ROS) and is brought about by a disruption of the physiological balance between normal oxidant production and various antioxidant defense systems. The brain is particularly sensitive to ROS accumulation, and oxidative stress is implicated in the pathogenesis of many chronic neurodegenerative diseases as well as acute neuronal injury such as stroke (McCulloch and Dewar, 2001). It is noteworthy that oxidative stress alters many metabolic and signaling pathways through effects on protein redox state and indirectly through triggering the release of intracellular stores of metal ions such as Zn^{2+} (Sensi and Jeng, 2004). Zn^{2+} has been found to be toxic to neurons in vitro (Koh and Choi, 1994), and intracellular Zn^{2+} accumulation plays a crucial role in ischemic injury (Koh et al., 1996) as well as other forms of neuronal cell death (Land and Aizenman, 2005).

Several cellular signaling pathways are activated by oxidative stress in neurons, including the mitogen-activated protein kinases (MAPKs). MAPK members, including extracellular signal-regulated kinase (ERK) 1/2, Jun NH_2-terminal kinase (JNK)/stress-activated protein kinase, and p38 MAPK kinase families, affect a variety of neuronal cell functions (Thomas and Huganir, 2004). The JNK/stress-activated protein kinase and p38 pathways are most often associated with neuronal cell death, whereas ERK1/2 contributes to

This work was supported by National Institutes of Health grants NS38319 (to D.B.D.) and NS43277 (to E.A.)

Y.H. and R.S. contributed equally to this work and are considered co-first authors.

Article, publication date, and citation information can be found at http://molpharm.aspetjournals.org.
doi:10.1124/mol.108.049064.

ABBREVIATIONS: ROS, reactive oxygen species; MAPK, mitogen-activated protein kinase; ERK, extracellular signal-regulated kinase; JNK, Jun NH_2-terminal kinase; PI, propidium iodine; HCA, homocysteate; MEK, mitogen-activated protein kinase kinase; U0126, 1,4-diamino-2,3-dicyano-1,4-bis(methylthio)butadiene; PP2A, protein phosphatase-type 2A; IP, immunoprecipitation; PAGE, polyacrylamide gel electrophoresis; PBST, phosphate-buffered saline with Tween 20; BSA, bovine serum albumin; TPEN, *N*,*N*,*N*′,*N*′-tetrakis-(2-pyridylmethyl)-ethylenediamine; AM, acetoxymethyl ester; MRE, metal regulatory element; DSP, dual-specificity protein phosphatase; BHA, butylated hydroxyanisole; TNF, tumor necrosis factor; MKP, mitogen-activated protein kinase phosphatase; DTT, dithiothreitol; p, phosphorylated.

neuroprotection and survival (Xia et al., 1995). However, ERK1/2 has also been found to promote neuronal cell death in several in vitro models of neurodegeneration induced by oxidative stress (Satoh et al., 2000; Levinthal and Defranco, 2004) or Zn^{2+} (Seo et al., 2001). In fact, pharmacological inhibition of ERK1/2 activation in vivo reduces neuronal cell injury in response to transient focal ischemia (Alessandrini et al., 1999).

Glutamate-induced oxidative toxicity in the HT22 neuroblastoma cell line (Li et al., 1997) and primary immature cortical neurons (Murphy et al., 1990) has provided a useful model for studying the effects of oxidative stress on neuronal cell death. Both HT22 cells and immature neurons lack *N*-methyl-D-aspartate receptors but are depleted of glutathione upon glutamate-mediated inhibition of a glutamate/cystine antiporter (Murphy et al., 1990). Oxidative stress in HT22 cells and immature neurons triggers a form of cell death that has features of both apoptosis and necrosis (Li et al., 1997; Tan et al., 2001).

We have reported previously that oxidative stress in HT22 cells and immature neurons causes a biphasic activation of ERK1/2 with the delayed, sustained activation of ERK1/2 contributing to neuronal cell death (Stanciu and DeFranco, 2002; Luo and DeFranco, 2006). This sustained activation of ERK1/2 is mediated primarily by a selective, reversible inhibition of ERK1/2-directed phosphatases (Levinthal and Defranco, 2005). In this study, we show that increased intracellular accumulation of Zn^{2+} in oxidatively stressed neuronal cells is responsible for the selective inhibition of ERK-phosphatases and ensuing ERK1/2 activation and cell death. We were surprised to find that ERK1/2 also functions to maintain elevated levels of Zn^{2+}. Thus, the elevation of intracellular Zn^{2+} within damaged neurons can trigger a robust positive feedback loop operating through activated ERK1/2 that rapidly sets into motion a Zn^{2+}-dependent pathway of cell death.

Materials and Methods

Primary Neuron Cultures and Cell Lines. Primary neuron cultures were prepared from the cortices of embryonic 17 Sprague-Dawley rat fetuses (Hilltop Lab Animals, Scottsdale PA). In brief, the cortices of embryonic 17 Sprague-Dawley rat fetuses were dissected and dissociated by repeated triturating in Hanks' balanced salt solution (5.4 mM KCl, 0.3 mM Na_2HPO_4, 0.4 mM KH_2PO_4, 4.2 mM $NaHCO_3$, 137 mM NaCl, and 5.6 mM D-glucose, pH 7.4) without Ca^{2+} or Mg^{2+} (Invitrogen, Carlsbad CA). The cell suspensions were then passed through a 40-μm cell strainer (BD Biosciences, San Jose, CA) to remove clumped cells. Cells were then counted and plated on 50 μg/ml poly-D-lysine-coated cultures plates at a density of $\sim 1 \times 10^5$ cells/cm^2. Cell viability was assessed by the uptake of trypan blue dye and was usually greater than 80%. Cultures were maintained for 2 to 3 days in media [Dulbecco's modified Eagle's medium and 10% fetal calf serum (HyClone Laboratories, Logan UT), 10% Ham's F-12 nutrient supplement (Sigma-Aldrich, St. Louis MO), 1.9 mM glutamine, 24 mM HEPES buffer, and 4.5 mg/ml glucose] at 37°C and 5% CO_2. At this time, the mixed cortical cultures are ~80% neuronal, with ~20% glial fibrillary-associated protein-staining cells (Murphy et al., 1990). HT22 cells were maintained in Dulbecco's modified Eagle's medium supplemented with 10% fetal bovine serum, 100 units of penicillin, and 100 μg/ml streptomycin at 37°C and 5% CO_2.

Cell Viability Assay. A DNA dye propidium iodide (PI) was used to assess cell viability. PI is excluded from healthy, intact cells and could only gain access into cells with a compromised plasma membrane. Fourteen to 16 h after being treated with homocysteate (HCA), primary neurons were incubated for 10 min in media containing a final concentration of 6.25 μg/ml PI. Cells were observed under an inverted fluorescence microscope equipped with phase-contrast optics (Nikon Eclipse TE200; Nikon, Melville, NY). Multiple fields were counted for each condition in at least three independent cultures with the total cells population of at least 500 neurons each condition. Toxicity was assessed in 5 mM glutamate-treated HT22 cells at 12 h by using the PI staining method described above.

ERK2- and JNK3-Directed Phosphatase Activity Assay. A nonradioactive method has been modified for determining ERK2- and JNK3-directed phosphatase activity in cell lysates, and it is based on detecting dephosphorylation of a purified, dual-phosphorylated, His_6-tagged ERK2 or JNK3 upon incubation with the cell lysates (Levinthal and Defranco, 2005). The alterations of ERK2 or JNK3 phosphatase activity within the cell lysates can be monitored by measuring changes in the phosphorylation state of the isolated phosphorylated ERK2 or JNK3 substrate, as shown by Western blotting with a phospho-specific ERK1/2 or JNK antibody. In brief, 150 μg of cell lysates were diluted into a total volume of 250 μl in phosphatase assay buffer (10 mM $MgCl_2$, 10 mM HEPES, pH 7.5 and 10 μM U0126, a MEK inhibitor). Recombinant dual-phosphorylated His_6-ERK2 or His_6-JNK3 (BIOMOL Research Laboratories, Plymouth Meeting, PA) was added to each sample (30 ng/sample), and the reactions were maintained at 37°C for 15 min where indicated. For the in vitro Zn^{2+} inhibition experiment, different concentrations of $ZnCl_2$ were preincubated with cell lysates for 10 min at 37°C before the addition of purified pERK2 substrate. After a 15-min incubation at 37°C, reactions were stopped by the addition of 250 μl of wash buffer (8 M urea, pH 8.6, containing 10 mM imidazole). Then, 30 μl of Ni^{2+}-conjugated, magnetic beads (QIAGEN, Valencia CA) was added to each reaction. After 90 min of rocking at 4°C, the samples were washed twice with wash buffer followed by one wash in 300 mM NaCl and 25 mM Tris, pH 7.5. The beads were then suspended in Laemmli sample buffer, boiled for 5 min, loaded onto a 10% polyacrylamide gel, transferred to a polyvinylidene fluoride membrane (Millipore Corporation, Billerica, MA) and subjected to Western blotting to detect phosphorylated ERK1/2, total ERK1/2, phosphorylated JNK3, or total JNK3.

PP2A Phosphatase Assay. The immunoprecipitation (IP) assay for PP2A activity was performed using procedures outlined in a PP2A IP assay kit (Millipore Corporation). In brief, PP2A was immunoprecipitated from HT22 cell lysates prepared in a PP2A phosphatase assay lysis buffer by using a monoclonal antibody against the C subunit of PP2A. A sample of the immunoprecipitate was analyzed for recovery of PP2A C subunit by Western blotting. PP2A activity in the remainder of the immunoprecipitates was measured using a synthetic phosphopeptide substrate and a malachite green detection system for released phosphate (Millipore Corporation). Activity measurements expressed as picomoles of phosphate released were normalized to total PP2A C subunit recovered within individual immunoprecipitates.

Western Blot Analysis. Cells were treated with HCA or glutamate, scraped, collected in 1× phosphate-buffered saline, and then centrifuged at 7000 rpm for 3 min. The pellets were then disrupted in lysis buffer (50 mM Tris-Cl, pH 7.5, 2 mM EDTA, 100 mM NaCl, and 1% Nonidet P-40, supplemented with protease inhibitor (Protease inhibitor cocktail; Sigma-Aldrich). The solubilized lysates were then centrifuged at 13,000 rpm for 5 min at 4°C, and supernatants were collected for further analysis. Protein concentrations of the extracts were determined using the Bio-Rad reagent (Bio-Rad, Hercules, CA). Equivalent amount of total protein (20–30 μg) were separated by SDS-PAGE on 10% polyacrylamide gels and then transferred to polyvinylidene membranes. Membranes were blocked with 5% dry milk in phosphate-buffered saline/0.1% (v/v) Tween 20 (PBST) for 1 h at room temperature. Membranes were then incubated with primary antibodies (anti-phospho-ERK1/2, anti-total ERK1/2, anti-phospho-JNK, anti-total JNK, all from Cell Signaling

Technology (Danvers MA) overnight at 4°C with 2% BSA in PBST. The membranes were then washed three times with PBST (10 min each time), incubated with the appropriate horseradish peroxidase-conjugated secondary antibody for 40 min at room temperature, and followed by three washes with PBST. Immunoreactive bands were then revealed by enhanced chemiluminescence (GE Healthcare, Chalfont St. Giles, Buckinghamshire, UK) using standard X-ray film (Carestream Health, Rochester, NY). Densitometry was performed using a Personal Densitometer SI (GE Healthcare) linked to the ImageQuant 5.2 software (GE Healthcare).

Intracellular Zinc Imaging. Neuronal cultures were incubated in a 5 μM Fluozin 3-AM (Invitrogen, Carlsbad CA)-containing solution composed of HEPES-buffered saline, supplemented with 5 mg/ml BSA, for approximately 30 min. Immediately after incubation, coverslips were submerged in a recording chamber (Warner Instruments, Hamden CT) mounted on an inverted epifluorescence microscope (Nikon Eclipse TE200) equipped with a 10× and a 20× objective. Minimal essential medium-HEPES-BSA was continuously perfused through the recording chamber via a gravity-driven perfusion system. Using a computer-controlled monochromator (Polychrome II; TILL Photonics, Aachen, Germany) and a charge-coupled device camera (IMAGO; TILL Photonics), images were acquired with 490-nm excitation light. Once a series of baseline fluorescence images were established, a 20 μM tetrakis-(2-pyridylmethyl)ethylenediamine (TPEN) solution was perfused through the chamber to chelate intracellular zinc and quench the fluorescent signal. The relative fluorescence for all cells (n = 6–40) was determined by subtracting the TPEN-quenched signal from the initial fluorescence, and an average value was calculated for each coverslip (n = 6). Data were analyzed and plotted using Origin 6.0 (OriginLab Corp., Northampton MA).

Transfection and Luciferase Assay. Transfection of HT22 cells was performed with Lipofectamine 2000 as described previously (Hara and Aizenman, 2004). HT22 cells were cotransfected with a firefly luciferase-containing plasmid driven by four tandem metal regulatory element (MRE) sequences (Hara and Aizenman, 2005) and a constitutively expressed *Renilla reniformis* luciferase plasmid (pRLTK), which serves as an internal control. Twenty-four hours after transfection, cells were stimulated with 5 mM glutamate alone or in the presence of 1 μM TPEN for 6 h. Cells were then incubated overnight with the nonselective cysteine protease inhibitor bocaspartyl (OMe)-fluoromethylketone (20 μM) to minimize oxidative damage to the cells and maximize MRE-driven expression. Firefly and *R. reniformis* luciferase activity were then measured using the Dual-Glo assay system (Promega, Madison, WI).

Statistics. Comparison of two means was performed using a paired t test. Comparison of multiple mean values was performed by analysis of variance with either Tukey's or Bonferroni's post hoc tests for significance. p values <0.05 were considered to be significant. All data were analyzed using Prism version 4.0 for Windows (GraphPad Software, Inc., San Diego CA).

Results

ERK2-Directed Phosphatase Activity Is Inhibited during Oxidative Toxicity in HT22 Cells and Immature Neurons. We had previously reported that glutamate-induced oxidative stress in immature neurons inhibits ERK2-directed phosphatases resulting in sustained activation of ERK1/2 (Levinthal and Defranco, 2005). Because HT22 cells exhibit analogous ERK1/2-dependent oxidative toxicity, we first set out to examine whether ERK1/2-directed phosphatases were inhibited by glutamate treatment in HT22 cells analogous to previously published results in immature neurons (Levinthal and Defranco, 2005). An in vitro phosphatase assay was therefore used with whole cell lysates to dephosphorylate purified, dual-phosphorylated, His_6-tagged ERK2 (Levinthal and Defranco, 2005). A nonspecific dual-specificity protein phosphatase (DSP), λ protein phosphatase, was used as a positive control for ERK2 dephosphorylation (Fig. 1A).

As shown in Fig. 1A, whole cell lysates prepared from HT22 cells possess robust ERK2 phosphatase activity, which was decreased upon a 7.5-h glutamate treatment of the cells (Fig. 1A). All phosphatase assays reported in this manuscript were performed after lengths of glutamate (or HCA) treatment that did not lead to overt signs of cell death (e.g., rounding and loss of adherence) but that were sufficient to generate oxidative stress (Levinthal and Defranco, 2005). Quantification of four independent experiments revealed a significant increase ($p < 0.05$) in the normalized levels of phosphorylated ERK2 in HT22 cell lysates exposed to glutamate for 7.5 h compared with untreated cultures (Fig. 1B). When cells were exposed to shorter treatments with glutamate (i.e., 2 and 5 h), ERK2 phosphatase activity was not significantly affected (Fig. 1A). The length of glutamate exposure that leads to inhibition of ERK2 phosphatase activity in HT22 cells is coincident with that required for maximal oxidative and enhanced ERK1/2 phosphorylation (Stanciu et al., 2002).

To confirm the effect of glutamate on the inhibition of ERK2 phosphatase activity in immature neurons, we used the glutamate analog HCA to induce oxidative stress. HCA is a glutamate analog that has a relatively high binding affinity to glutamate/cysteine antiporter. Although glutamate has been widely used to induce oxidative toxicity to immature neurons, we and others (Ryu et al., 2003) have found that HCA generates more reliable and reproducible toxicity and less variation between neuronal cultures. The ERK2 phosphatase assay was performed with whole cell lysates prepared from cultures treated with HCA for different times (i.e., 12, 14, and 16 h). As shown in Fig. 1C, a 14- or 16-h treatment of neurons with HCA led to the inhibition of ERK2 phosphatase activity (Fig. 1, C and D).

Phosphorylated ERK1/2 is a substrate for various phosphatases, including members of the protein serine/threonine phosphatase (PSTP) and DSP families (Farooq and Zhou, 2004). In fact, glutamate treatment of HT22 cells and immature neurons was recently shown to trigger the degradation of the DSP MKP1 (Choi et al., 2006), which we confirmed in our cells (data not shown). However, because the inhibition of ERK1/2 phosphatase activity in glutamate-treated immature neurons is reversible (Levinthal and Defranco, 2005), global degradation of ERK1/2 phosphatases is not solely responsible for persistent ERK1/2 activation. We therefore used IP to selectively analyze the effects of glutamate on the activity of PP2A, a PSTP that is one of the predominant ERK1/2 phosphatases expressed in neurons (Levinthal and Defranco, 2005). As shown in Fig. 1E, glutamate treatment of HT22 cells led to a significant decrease in PP2A activity, when normalized for total PP2A catalytic subunit recovered in immunoprecipitates. The levels of PP2A catalytic subunit in HT22 cells were not reduced upon glutamate treatment (Fig. 1E). Therefore, oxidative stress in neurons may limit ERK1/2 phosphatase activity by effecting either select phosphatase expression (e.g., MKP1) (Choi et al., 2006) or activity (e.g., PP2A).

An Antioxidant That Blocks Oxidative Toxicity Reduces ERK1/2 Activation and Restores ERK2 Phosphatase Activity. The antioxidant butylated hydroxyanisole

(BHA) protects against glutamate-induced oxidative toxicity in immature neurons (Ryu et al., 2003) and HT22 cells (data not shown). BHA also prevents the oxidative stress-induced inhibition of JNK phosphatases and tumor necrosis factor (TNF)-α induced cell death in fibroblast cell lines (Kamata et al., 2005). The effects of BHA in blocking ERK1/2 activation induced by oxidative stress has also been observed in other cell types such as head and neck squamous carcinoma cell (Kim et al., 2006a). We therefore used BHA to assess whether ERK1/2 activation and the inhibition of ERK2-directed phosphatase activity is mediated by ROS.

As shown in Fig. 2A, a 7.5-h glutamate treatment induced significant ERK1/2 activation in HT22 cells. In immature neurons, HCA activation of ERK1/2 was evident at 14 h and peaked at 16 h (Fig. 2B), analogous to the time course of ERK1/2 activation by glutamate in immature neurons (Stanciu et al., 2002; Levinthal and Defranco, 2005). The administration of BHA blocked ERK1/2 activation induced by oxidative stress in HT22 cells and neurons (Fig. 2, A and B).

To investigate the mechanism responsible for BHA inhibition of ERK1/2 activation, ERK2 phosphatase assays were performed using cell lysates prepared from oxidatively stressed HT22 cells and neurons. As shown in Fig. 2, C and E, BHA prevented the inhibition of ERK2 phosphatase activity after glutamate treatment in HT22 cells. Likewise, BHA abrogated the inhibition of ERK phosphatase activity in neurons subject to HCA treatment (Fig. 2, D and F). Thus, ROS-mediated inhibition of protein phosphatase activity is responsible, in part for the activation of ERK1/2 in oxidatively stressed neurons.

Selective Inhibition of ERK2 Phosphatase Activity by Zn^{2+} in Neuronal Cell Extracts. ERK1/2 phosphatases such as MKPs and PP2A are reversibly inactivated by thiol oxidation (Foley et al., 2004). We found previously that ERK2 phosphatase activity in extracts prepared from oxidatively stressed neurons was restored by the in vitro addition of DTT (Levinthal and Defranco, 2005). Thus, oxidative inhibition of ERK1/2 phosphatases in HT22 cells and primary cortical neurons may occur through direct or indirect thiol oxidation of the phosphatases. However, DTT in addition to its well known thiol-reducing properties is also an effective Zn^{2+} chelating agent (Cornell and Crivaro, 1972). Thus, restoration of ERK2 phosphatase activity in extracts prepared from oxidatively stressed neurons by DTT may not be due solely to reduction of oxidized thiols. It is noteworthy that Zn^{2+} inhibits purified phosphatases that could act on ERK1/2, including the PSTP, PP2A (Zhuo and Dixon, 1997), and protein tyrosine phosphatases (Maret et al., 1999). As such, we investigated the effect of Zn^{2+} on ERK2 phosphatase activity.

As shown in Fig. 3A, a 10-min preincubation of HT22 cell lysates with $ZnCl_2$ caused a concentration-dependent inhibition of ERK2 phosphatase activity, with the maximal inhibi-

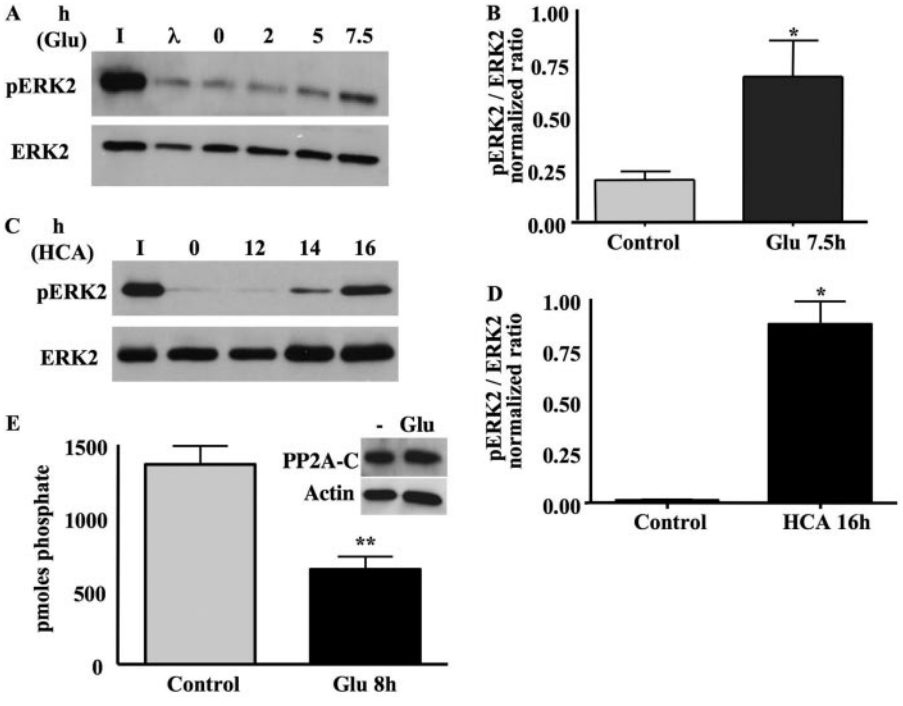

Fig. 1. ERK2 phosphatase activity is inhibited upon oxidative stress in HT22 cells and immature neurons. A, HT22 cells were treated with 5 mM glutamate for 0, 2, 5, or 7.5 h. Whole cell lysates were incubated with purified, phosphorylated ERK2 (pERK2), and phosphatase activity was assessed by Western blots that revealed pERK2 or total ERK2. I, phosphatase assay input; λ, lambda phage protein phosphatase (positive control). B, quantification of the results from four independent experiments, revealing a significant decrease in ERK2 phosphatase activity after glutamate-induced oxidative stress in HT22 cells (mean ± S.E.M.; $n = 4$). *, $p < 0.05$. C, ERK2 phosphatase activity is inhibited upon 5 mM HCA treatment immature neurons. Immature neurons were treated with HCA for 0, 12, 14, or 16 h. Whole cell lysates were incubated with purified pERK2, and phosphatase activity was assessed by Western blots that revealed either pERK2 or total ERK2. I, phosphatase assay input. D, quantification of the results from three independent experiments, revealing a significant decrease in ERK2 phosphatase activity after HCA-induced oxidative stress in immature neurons (mean ± S.E.M.; $n = 3$). *, $p < 0.05$. E, PP2A phosphatase activity in immunoprecipitates from HT22 cell extracts. PP2A was recovered by immunoprecipitation from whole cell lysates prepared from either untreated or 5 mM glutamate-treated (8 h) HT22 cells, and phosphatase activity was assayed using a synthetic phosphopeptide substrate. Activity normalized to PP2A C subunit recovered in immunoprecipitates is expressed as picomoles of phosphate removed (mean ± S.E.M.; $n = 3$; **, $p < 0.01$). Inset, representative Western blot analysis of PP2A C subunit and β-actin expression in glutamate-treated (8 h) HT22 cells.

tion observed at 10 μM. It must be noted, however, that the actual concentration of "free" Zn^{2+} is likely to be much lower that what we have added by way of the various constituents of the cell extract and assay buffer that would bind to this metal. Therefore, it is possible that the actual inhibitory concentrations of Zn^{2+} are very low, even in the nanomolar range (Frederickson et al., 2006). Quantification of several independent experiments revealed a significant inhibition of ERK2 phosphatase activity by added zinc at 10 μM (Fig. 3B; $p < 0.01$). ERK2 phosphatase activity measured in HT22 cell extracts is not sensitive to Fe^{2+} (Fig. 3C), another metal associated with oxidative toxicity in HT22 cells and immature cortical neurons (Zaman et al., 1999). This result is consistent with studies establishing stimulatory effects of

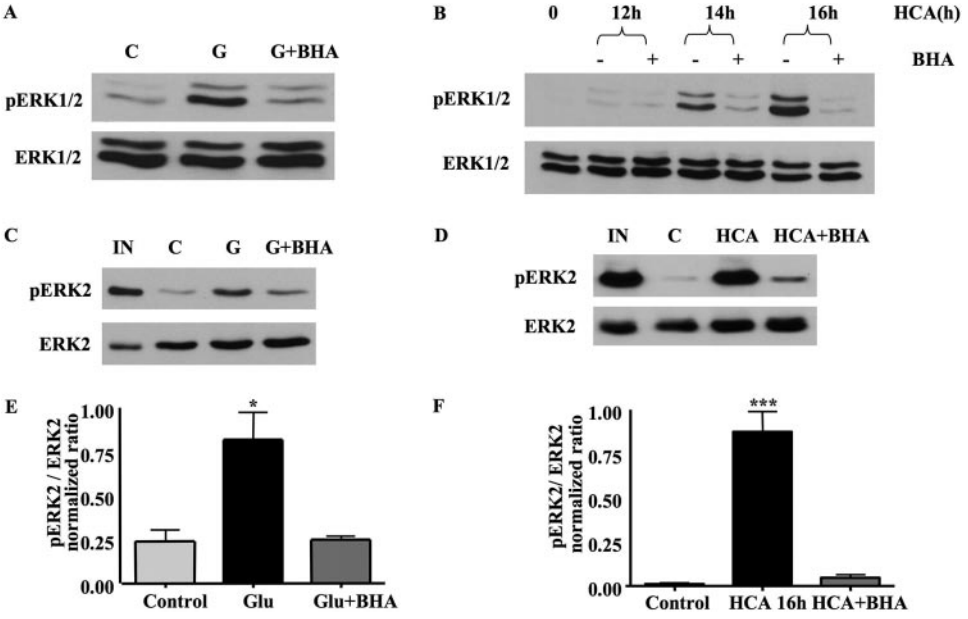

Fig. 2. BHA blocks ERK1/2 activation and the inhibition of ERK2 phosphatase activity induced by oxidative stress in HT22 cells and immature neurons. A, HT22 cells were treated with glutamate or glutamate plus 100 μM BHA for 7.5 h. Then, 20 μg of total protein lysate was separated by SDS-PAGE and subjected to Western blot analysis to detect pERK1/2 and total ERK1/2 on the same blots. C, control cell lysates. The addition of BHA blocked ERK1/2 activation after glutamate-induced oxidative stress. B, immature neurons were treated with HCA for 0, 12, 14, or 16 h in the presence or absence of BHA. Then, 20 μg of total protein lysate was separated by SDS-PAGE and subjected to Western blot analysis to detect pERK1/2 and total ERK1/2 on the same blots. The administration of BHA significantly blocks ERK1/2 activation after HCA treatment. C, whole cell lysates prepared from control untreated (C), glutamate (G)-treated, or glutamate plus BHA-treated HT22 cells were incubated with purified pERK2, and phosphatase activity was assessed by Western blot that revealed either pERK2 or total ERK2. IN, ERK2 input. The addition of BHA reverses the glutamate-induced inhibition of ERK2 phosphatase activity. D, whole cell extracts prepared from the control (C), HCA-treated, and HCA plus BHA-treated immature neurons were incubated with purified pERK2, and phosphatase activity was assessed by Western blot that revealed either pERK2 or total ERK2. IN, ERK2 input. The administration BHA reverses the inhibition of ERK2 phosphatase activity after HCA-induced oxidative toxicity. E, quantification of the results from three independent experiments. Coadministration of BHA abrogates the inhibition of ERK2 phosphatase activity in glutamate-treated HT22 cells (mean ± S.E.M.; $n = 3$). *, $p < 0.05$. F, quantification of the results from three independent experiments. Coadministration of BHA abrogates the inhibition of ERK2 phosphatase activity in HCA-treated immature neurons (mean ± S.E.M.; $n = 3$). ***, $p < 0.001$.

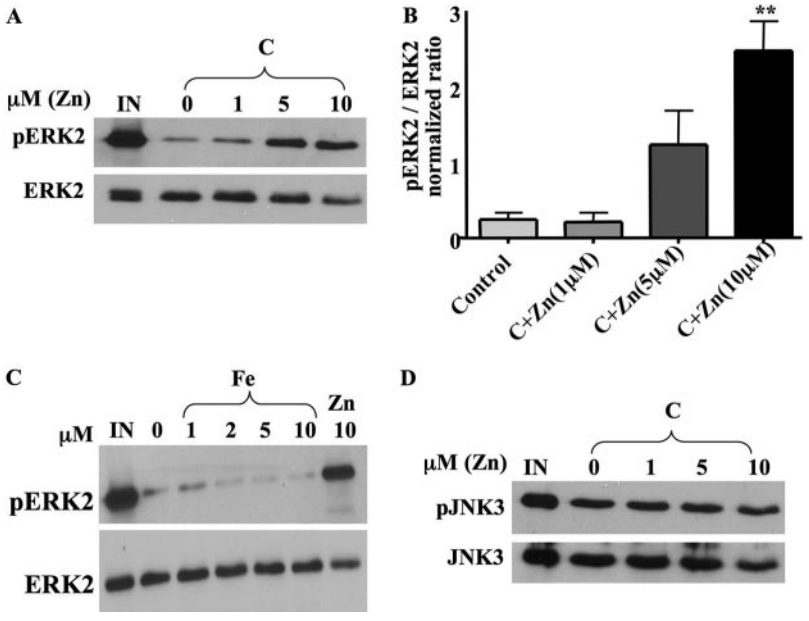

Fig. 3. Zn^{2+} specifically inhibits ERK2 phosphatase activity in neuronal cell extracts. A, various concentrations of $ZnCl_2$ were preincubated with whole cell lysates prepared from untreated HT22 cells for 10 min at 37°C before the addition of pERK2 substrate. ERK2 dephosphorylation was monitored by Western blot analysis as described in Fig. 2. B, quantification of the results from three independent experiments. $ZnCl_2$ at 10 μM significantly inhibits ERK2 phosphatase activity in HT22 cells (mean ± S.E.M.; $n = 3$). **, $p < 0.01$. C, various concentrations of $FeCl_2$, and 10 μM $ZnCl_2$ as a control, were preincubated with whole cell lysates prepared from untreated HT22 cells for 10 min at 37°C before the addition of pERK2 substrate. ERK2 dephosphorylation was monitored by Western blot analysis as described previously. D, various concentrations of $ZnCl_2$ were preincubated with whole cell lysates prepared from untreated HT22 cells for 10 min at 37°C before the addition of pJNK3 substrate. JNK3 dephosphorylation was monitored by Western blot analysis as described previously. $ZnCl_2$ does not inhibit JNK3 phosphatase activity in HT22 cell extracts.

Fe^{2+} on PP2A (Yu, 1998), the major ERK2 phosphatase reversibly affected by glutamate in HT22 cells (Fig. 1E).

To determine whether the Zn^{2+} inhibition of phosphatase activity is specific to ERK phosphatases, we then examined Zn^{2+} effects on JNK3 phosphatase activity. As shown in Fig. 3D, $ZnCl_2$ did not affect JNK3 phosphatase activity in HT22 cell lysates, suggesting that exogenous Zn^{2+} is selective in inhibiting ERK2-directed phosphatases in HT22 cell extracts. This is not surprising because oxidative toxicity in HT22 cells and immature neurons is not associated with an increase in JNK activation or an inhibition of JNK phosphatase activity (Levinthal and Defranco, 2005). Furthermore, active p38 MAPK is not detected in unstimulated or glutamate-treated HT22 cells (Levinthal and Defranco, 2005).

HT22 cells were also treated with $ZnCl_2$ to establish whether Zn^{2+} can be directly responsible for ERK1/2 activation in vitro irrespective of oxidative stress. As shown in Fig. 4A treatment of HT22 cells with 10 μM $ZnCl_2$ in the presence of the Zn^{2+} carrier sodium pyrithione (i.e., at 5 μM) led to a rapid and robust increase in ERK1/2 phosphorylation. This rapid ERK1/2 activation is not due to secondary generation of ROS, because it was not affected by the addition of the antioxidant BHA (Fig. 4B). Finally, rapid Zn^{2+}-dependent, ROS-independent ERK1/2 activation was associated with an inhibition of ERK2 phosphatase activity in HT22 cell lysates (Fig. 4C), confirming a direct role for Zn^{2+} in phosphatase inhibition.

Oxidative Stress Triggers Zn^{2+} Accumulation in HT22 Cells and Primary Neurons. The affect of oxidative stress in HT22 cells and immature neurons on intracellular Zn^{2+} accumulation was assessed using FluoZin 3-AM, a fluorescent Zn^{2+} indicator dye (Devinney et al., 2005). Relative intracellular Zn^{2+} levels was obtained by quantitative measures of FluoZin 3-AM fluorescence within individual cells that is quenchable by the Zn^{2+} chelator TPEN (Knoch et al., 2008). As shown in Fig. 5A, oxidative stress in HT22 cells and immature neurons led to a doubling of the relative TPEN-quenchable FluoZin 3-AM fluorescence. Thus oxidative stress in both HT22 cells and immature neurons trigger the accumulation of intracellular Zn^{2+}, similar to what we have reported in other systems (Aizenman et al., 2000; Zhang et al., 2004).

To confirm these findings, we used a molecular assay that measures specific Zn^{2+}-driven gene expression. HT22 cells were transfected with a firefly luciferase-containing plasmid driven by four tandem MRE sequences (Hara and Aizenman, 2004). The MRE sequence is found in Zn^{2+}-regulated genes, including metallothionein. MRE-driven gene expression is activated after the binding of Zn^{2+} to the metal regulatory element transcription factor-1 transcription factor-1. As shown in Fig. 5A, inset, MRE-driven luciferase expression was significantly increased in the glutamate-treated cells, whereas this effect was abrogated by TPEN. This result strongly indicates that during glutamate-induced oxidative stress, sufficient intracellular Zn^{2+} was liberated to trigger metal regulatory element transcription factor-1/MRE-driven gene expression.

To determine the relationship between oxidant production, intracellular Zn^{2+} accumulation, and ERK1/2 activation, neurons were exposed to HCA in the presence or absence of either the antioxidant BHA or the MEK1/2 inhibitor U0126. As shown in Fig. 5B, BHA blocked HCA-induced intracellular Zn^{2+} accumulation and exerted no significant effect on the relative intracellular Zn^{2+} levels when given alone. It is noteworthy that U0126 treatment also reduced TPEN-quenchable Zn^{2+} fluorescence in HCA-treated neurons and did not alter Zn^{2+} levels when given alone (Fig. 5B). Thus, Zn^{2+} accumulation triggered by ROS may be exacerbated through a positive feedback loop driven by activated ERK1/2.

Chelation of Intracellular Zn^{2+} Blocks ERK1/2 Activation and Restores ERK2 Phosphatase Activity. Zn^{2+}-induced ERK1/2 activation has been reported to contribute to neuronal cell death (Seo et al., 2001; Zhang et al., 2004). To

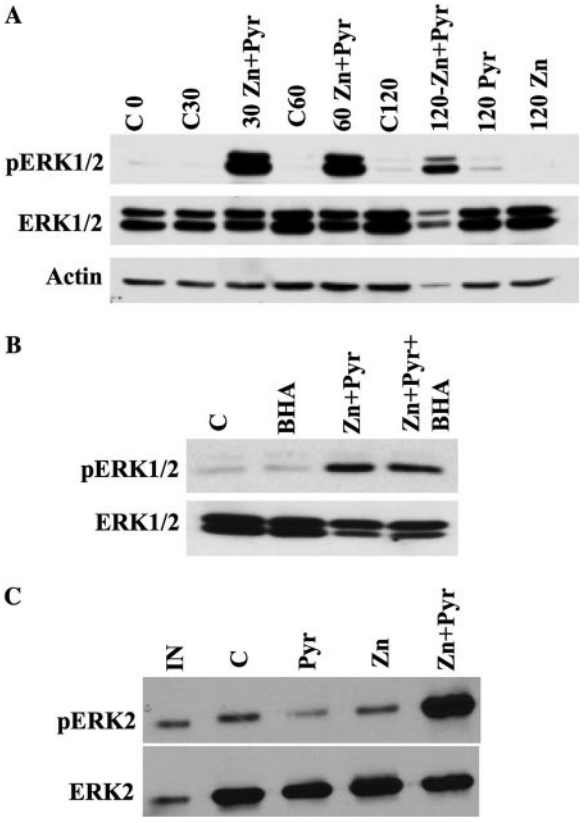

Fig. 4. Zn^{2+} triggers ERK1/2 activation through direct inhibition of ERK1/2 phosphatases in the absence of oxidative stress. A, HT22 cells were treated with 10 μM $ZnCl_2$ (Zn), 5 μM sodium pyrithione (Pyr), or both compounds in serum-free medium for indicated times (30, 60, or 120 min) followed by a 30-min recovery in serum-containing medium before harvesting. Control (C) conditions were performed without any additions but with a change from serum-free to serum containing medium that occurred at time 0. Then, 20 mg of total protein lysate was separated by SDS-PAGE and subjected to Western blot analysis to detect pERK1/2, total ERK1/2, and actin on the same blots. Blot shown is representative of three separate experiments where differences between control conditions at each time point, and combined $ZnCl_2$ and sodium pyrithione treatment groups were statistically significant ($p < 0.015$). B, HT22 cells were treated for 30 min with either 100 mM BHA alone, $ZnCl_2$ and sodium pyrithione, or BHA plus $ZnCl_2$ and sodium pyrithione as described above, with a 30-min recovery in serum-containing medium. The blot shown is representative of three separate experiments in which differences between control and combined $ZnCl_2$ and sodium pyrithione treatment groups as well as $ZnCl_2$, sodium pyrithione, and BHA groups were statistically significant ($p < 0.01$). C, whole cell lysates prepared from control untreated (C) or HT22 cells treated with 10 μM $ZnCl_2$ (Zn), 5 μM sodium pyrithione (Pyr), or both compounds (i.e., 30 min followed by 30-min recovery) were incubated with purified pERK2 and phosphatase activity assessed by Western blots that revealed either pERK2 or total ERK2. IN, pERK2 input. ERK2 phosphatase activity is inhibited by exposure of HT22 cells to $ZnCl_2$ and pyrithione. The blot shown is representative of three separate experiments in which differences between control and combined $ZnCl_2$ and sodium pyrithione treatment groups were statistically significant ($p < 0.05$).

evaluate the role of Zn^{2+} accumulation in activating ERK1/2 in HT22 cells and primary neurons, we used the high-affinity Zn^{2+} chelator TPEN. HT22 cells were treated with glutamate, in the presence or absence of 1 and 5 μM TPEN for 8 h. Whole cell lysates were then subject to Western blot analysis to detect phosphorylated, activated ERK1/2. As shown in Fig. 6A, exposure of HT22 cells to glutamate induced a large increase in ERK1/2 phosphorylation that was unaffected by the addition of 1 μM TPEN. However, the addition of 5 μM TPEN significantly blocked glutamate-induced ERK1/2 activation (Fig. 6A). This result suggests that ERK1/2 activation is downstream of Zn^{2+} accumulation.

Similar experiments were then extended to immature neurons, which were treated with HCA, HCA plus 1 μM TPEN, and HCA plus 5 μM TPEN for 16 h. Analogous to results obtained in HT22 cells, addition of 5 μM but not 1 μM TPEN significantly blocked the activation of ERK1/2 after oxidative stress in primary neurons (Fig. 6B).

Given that Zn^{2+} inhibits ERK2 phosphatase activity in vitro (Fig. 3, A and B), we set out to examine whether TPEN inhibition of ERK1/2 activation occurs through the reversal of Zn^{2+}-mediated inhibition of ERK1/2 phosphatases. The ERK2 phosphatase assay was performed on whole cell lysates prepared from untreated HT22 cells, or cells treated with glutamate, glutamate plus 1 μM or 5 μM TPEN. As shown in Fig. 6, C and E, ERK2 phosphatase activity was decreased after treatment with glutamate. The addition of 1 μM TPEN to HT22 cells did not reverse this inhibitory effect of glutamate (Fig. 6, C and E). However, the addition of 5 μM TPEN significantly reversed the inhibition of ERK2 phosphatase activity in HT22 cells that were treated with glutamate (Fig. 6, C and E). Similar results were obtained in primary neurons (Fig. 6, D and F). These results suggest that TPEN blocks Zn^{2+}-induced ERK1/2 activation by reversing a Zn^{2+}-mediated inhibition of ERK1/2 phosphatase activity.

Because U0126 has been found to block Zn^{2+}accumulation in oxidatively stressed cells (Fig. 5), we sought to examine whether U0126 could also reverse the inhibition of ERK2 phosphatase activity. The ERK2 phosphatase assay were therefore performed on cell lysates prepared from untreated HT22 cells or cells treated with glutamate or glutamate plus U0126. As shown in Fig. 6, G and H, U0126 treatment of HT22 cells reversed the inhibition of ERK2 phosphatase activity induced by oxidative stress. This result reinforces the notion that activated ERK1/2 contributes to a positive feedback loop that maintains elevated levels of intracellular Zn^{2+} and persistent inhibition of ERK1/2 phosphatases.

TPEN Protects Neuronal Cells from Oxidative Toxicity. We then set out to examine whether TPEN could also limit cell death. Because Zn^{2+} is an essential metal, we limited TPEN treatment to less than 16 h in both HT22 cells and primary neurons. Prolonged exposure (i.e., 48 h) of HT22 cells and primary neurons to TPEN alone is toxic (data not shown). HT22 cells were treated for 12 h with glutamate, glutamate plus 1 μM TPEN, glutamate plus 5 μM TPEN as well as 1 μM TPEN and 5 μM TPEN alone. A PI staining method was then used to assess cell toxicity (Levinthal and Defranco, 2005). As shown in Fig. 7A, a significant proportion of HT22 cells stained positive for PI upon glutamate treatment. Cells treated with glutamate plus 1 μM TPEN exhibited a similar extent of cell death. However, a 5 μM TPEN treatment significantly protected HT22 cells from glutamate-induced cell death (Fig. 7A; $p < 0.001$). This neuroprotective effect is similar to that provided by U0126 (Fig. 7A). A 12-h treatment with 1 and 5 μM TPEN alone exhibited no toxicity in HT22 cells (Fig. 7A).

This paradigm was then extended to immature neurons. These cultures were subject to the same treatment as HT22 cells, and cell toxicity was assessed after treatment for 16 h. Similar to the results obtained in HT22 cells, a 16-h treat-

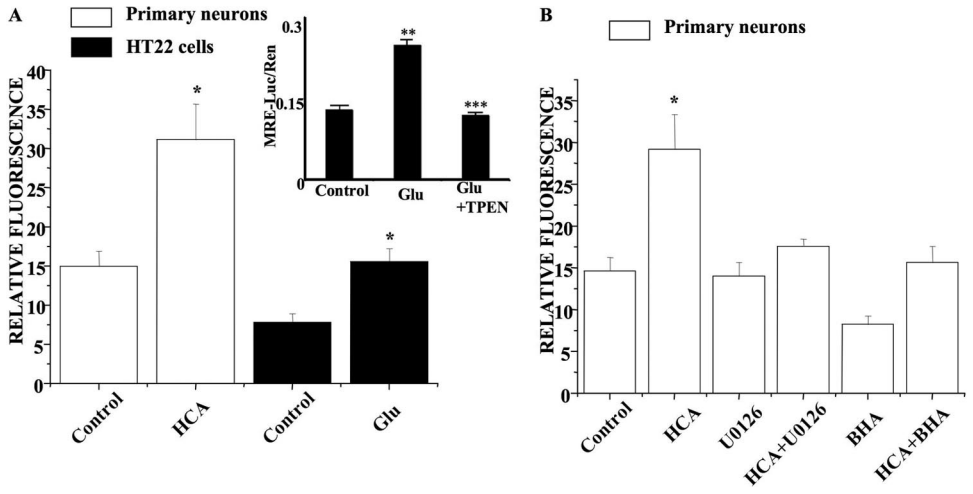

Fig. 5. Oxidative stress triggers zinc accumulation in HT22 cells and immature neurons. A, HT22 cells were treated with glutamate for 8 h, and immature neurons were treated with HCA for 12 h and loaded with FluoZin 3-AM for 30 min. The fluorescence imaging of intracellular zinc was then monitored by digital fluorescence microscopy, and relative fluorescence was measured. There is a significant increase in zinc accumulation after oxidative stress in both HT22 cells (mean ± S.E.M.; $n = 8$) and immature neurons (mean ± S.E.M.; $n = 6$). Inset, results of MRE-luciferase assay in HT22 cells that were either untreated (control), treated with 5 mM glutamate (Glu), or treated with 5 mM glutamate plus 5 μM TPEN. Values shown are the means ± S.E.M. of three experiments each performed in quadruplicate, with the firefly luciferase activity from the MRE-driven reported normalized to *R. reniformis* luciferase activity. Glutamate treatment leads to statistically significant (**, $p < 0.001$) difference in relative MRE-driven luciferase activity from control untreated cultures, whereas TPEN addition blocked the glutamate-induced increase in MRE-driven luciferase activity (***, $p < 0.001$). B, immature neurons were treated with HCA, HCA plus U0126, HCA plus BHA as well as U0126 only and BHA only, and then they were loaded with FluoZin 3-AM to measure the relative fluorescence. Coadministration with 10 μM U0126 (in dimethyl sulfoxide) decreases the zinc accumulation in HCA-treated immature neurons to basal levels (mean ± S.E.M.; $n = 6$). Likewise, the coadministration of 100 μM BHA also decreases the zinc release in HCA-treated immature neurons (mean ± S.E.M.; $n = 6$).

ment with HCA as well as HCA plus 1 μM TPEN induced significant cell death in immature neurons (Fig. 7B). However, the addition of 5 μM TPEN significantly protected immature neurons from HCA-induced toxicity (Fig. 7B). In summary, the dose of TPEN required to protect both HT22 cells and immature neurons from oxidative toxicity is coincident with that required to block ERK1/2 activation and ERK1/2 phosphatase inhibition.

The contribution of Fe^{2+} to neuronal oxidative toxicity was revealed previously with experiments demonstrating neuroprotective effects of Fe^{2+} chelation (Zaman et al., 1999). Because TPEN can also chelate Fe^{2+}, the metal selectivity of its neuroprotective actions was tested by the coapplication of TPEN with either Fe^{2+} or Zn^{2+}. As shown in Fig. 7C, inclusion of Zn^{2+} completely blocked the neuroprotective effect of TPEN in glutamate-treated HT22 cells ($p < 0.001$). In con-

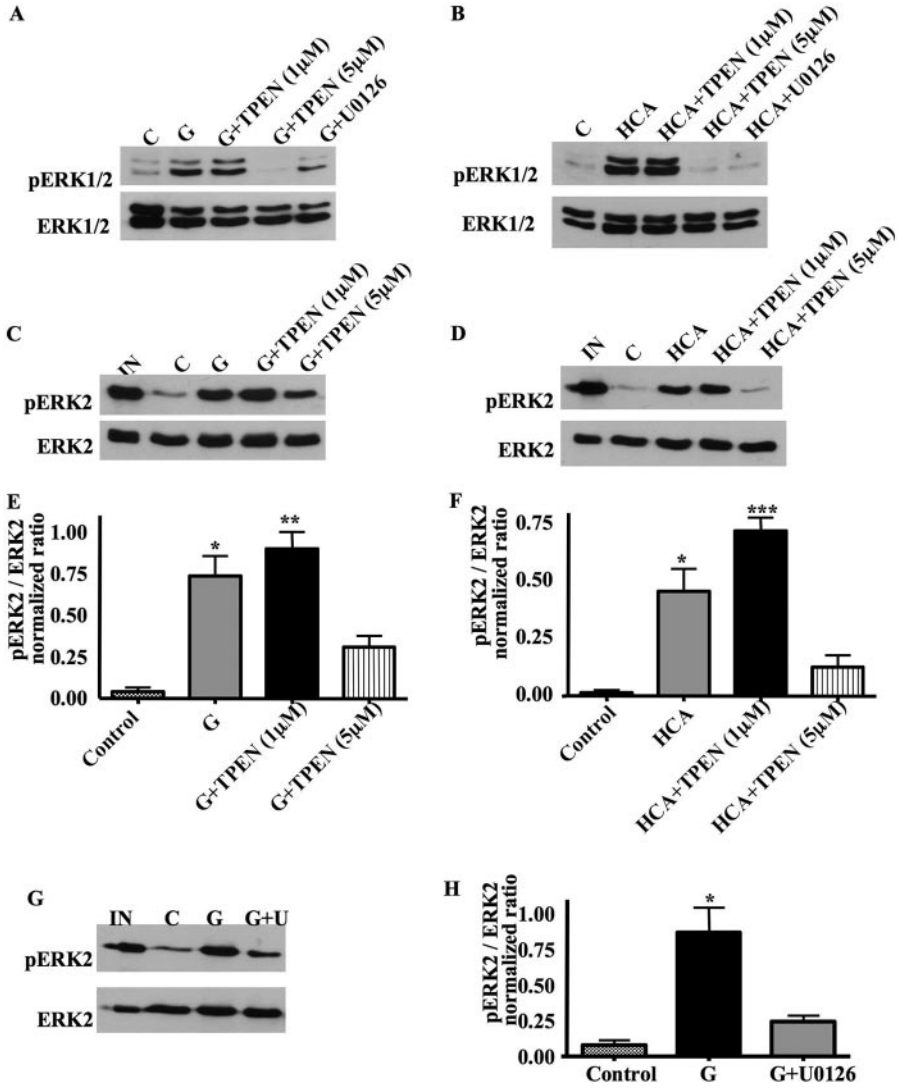

Fig. 6. TPEN blocks ERK1/2 activation and reverses the inhibition of ERK2 phosphatase activity after oxidative stress in HT22 cells and immature neurons. A, HT22 cells were treated with glutamate, glutamate plus 1 μM TPEN, glutamate plus 5 μM TPEN, or glutamate plus U0126 for 8 h. Then, 20 μg of total protein lysate was separated by SDS-PAGE and subjected to Western blot analysis to detect pERK1/2 and total ERK1/2 on the same blots. C, control cell lysates. TPEN (5 μM) blocks ERK1/2 activation after glutamate treatment in HT22 cells. B, immature neurons were treated with HCA, HCA plus 1 μM TPEN, HCA plus 5 μM TPEN, or HCA plus U0126 for 16 h. Then, 20 μg of total protein lysate was separated by SDS-PAGE and subjected to Western blot analysis to detect pERK1/2 and total ERK1/2 on the same blots. C, control cell lysates. TPEN (5 μM) blocks ERK activation after HCA treatment in immature neurons. C, an ERK2 phosphatase assay was performed on whole cell lysates prepared from untreated HT22 cells or from cells treated with glutamate, glutamate plus 1 μM TPEN, or glutamate plus 5 μM TPEN. TPEN reverses the inhibition of ERK2 phosphatase activity after glutamate treatment in HT22 cells. D, an ERK2 phosphatase assay was performed on whole cell lysates prepared from untreated immature neurons, or cells treated with HCA, HCA plus 1 μM TPEN, or HCA plus 5 μM TPEN. TPEN reverses the inhibition of ERK2 phosphatase activity after HCA treatment in primary immature cortical neurons. E, quantification of the ERK2 phosphatase activity results from three independent experiments in HT22 cells (mean $\pm$ S.E.M.; $n = 3$). There is significant difference between the group of glutamate-treated and glutamate plus 5 μM TPEN ($*$, $p < 0.05$) as well as between the group of glutamate plus 1 μM TPEN and glutamate plus 5 μM TPEN ($**$, $p < 0.01$). F, quantification of the ERK2 phosphatase assays results from three independent experiments in immature neurons (mean $\pm$ S.E.M.; $n = 3$). There is significant difference between the group of HCA-treated and HCA plus 5 μM TPEN ($*$, $p < 0.05$) as well as between the group of HCA plus 1 μM TPEN and HCA plus 5 μM TPEN ($***$, $p < 0.001$). G, an ERK2 phosphatase assay was performed on whole cell lysates prepared from untreated HT22 cells, or cells treated with glutamate, or glutamate plus 10 μM U0126. The administration of U0126 reverses the inhibition of ERK2 phosphatase activity after glutamate treatment in HT22 cells. H, quantification of the ERK2 phosphatase assay results from three independent experiments in HT22 cells (mean $\pm$ S.E.M.; $n = 3$). $*$, $p < 0.05$.

trast, addition of Fe^{2+} only partially reversed the actions of TPEN, suggesting that Zn^{2+} is a more important contributor to the oxidative toxicity observed in our system.

Discussion

ERK1/2 functions in many cell types to promote proliferation or survival but can also be diverted to participate in certain cell death pathways. For example, long-term activation of ERK1/2 is necessary for cell death induced by oxidative stress in immature neurons and HT22 cells (Satoh et al., 2000; Luo and DeFranco, 2006). In these cases, the inhibition of select protein phosphatases is primarily responsible for the persistent activation of ERK1/2 (Levinthal and Defranco, 2005). This conclusion was confirmed in a recent report, which also revealed the minimal contribution of upstream activating kinases (i.e., MEK1/2) to prolonged ERK1/2 activation in oxidatively stressed HT22 cells and immature neurons (Choi et al., 2006).

We show here that the inhibition of ERK1/2 phosphatases in HT22 cells and immature neurons subjected to glutathione depletion is indeed the result of oxidative stress, because phosphatase activity is restored in cells treated with BHA. This leads to reduced ERK1/2 activation and neuroprotection. The oxidative inhibition of protein phosphatase activity in TNF-α-treated fibroblasts is also eliminated by BHA treatment (Kamata et al., 2005). However, in TNF-α-induced oxidative toxicity and concanavalin A-induced liver toxicity in mice, cell death is associated with the selective inhibition of JNK phosphatases (Kamata et al., 2005). Glutamate-induced oxidative stress in immature neurons does not significantly affect JNK phosphatase activity (Levinthal and Defranco, 2005). Therefore, even though MAPK phosphatases are oxidant-sensitive, they are not globally inactivated by oxidative stress in cells. Depending upon the nature of the oxidative stress imposed upon living cells, select MAPK phosphatases may be protected from the damaging effects of reactive species because of their sequestration within subcellular compartments or multisubunit complexes that are inaccessible to short-lived oxidants.

Although several protein phosphatases are redox-sensitive and inhibited by direct thiol oxidation of a catalytic-site cysteine (Meng et al., 2002; Tonks, 2003), our results suggest that MAPK phosphatase activity may also be regulated in oxidatively stressed cells by the inhibitory effects of free Zn^{2+}. Zn^{2+} effects on ERK1/2 activation have been observed in neurons (Seo et al., 2001), but our results identify the molecular target of Zn^{2+} that is responsible for this effect. The sensitivity of various MAPK phosphatases to inhibition by Zn^{2+} was established with purified phosphatase preparations, suggesting that Zn^{2+} can act directly to impact the activity of these enzymes (Zhuo and Dixon, 1997). Zn^{2+}-mediated inhibition of protein tyrosine phosphatases has been suggested to affect insulin/insulin-like growth factor (Haase and Maret, 2003) or interleukin-8 (Kim et al., 2006b) signaling in C6 glioblastoma or BEAS-2B human airway epithelial cells, respectively. Thus, Zn^{2+}-mediated inhibition of protein phosphatase activity may not always be linked to cell death responses but could play a role in facilitating hormone signaling (Haase and Maret, 2003). However, prolonged inhibition of select MAPK phosphatases and ensuing persistent activation of specific MAPKs that drives toxicity in oxidatively stressed cells may reflect an inability to restore Zn^{2+} homeostasis (see below).

For PSTPs, Zn^{2+} may exert its inhibitory effects through the displacement of bound Mn^{2+} at the active site of their catalytic subunits (Zhuo and Dixon, 1997). It is noteworthy that purified PSTPs such as PP2A are refractory to exchange by Mn^{2+} once bound by Zn^{2+}; therefore, limited recovery of their activity can be achieved by Zn^{2+} chelation in vitro (Zhuo and Dixon, 1997). These potent inhibitory effects of Zn^{2+} on ERK1/2 phosphatases such as PP2A may explain the requirement for a 5 μM TPEN treatment to reverse the inhibition of ERK1/2 phosphatase activity in oxidatively stressed HT22 cells and immature neurons. It is noteworthy

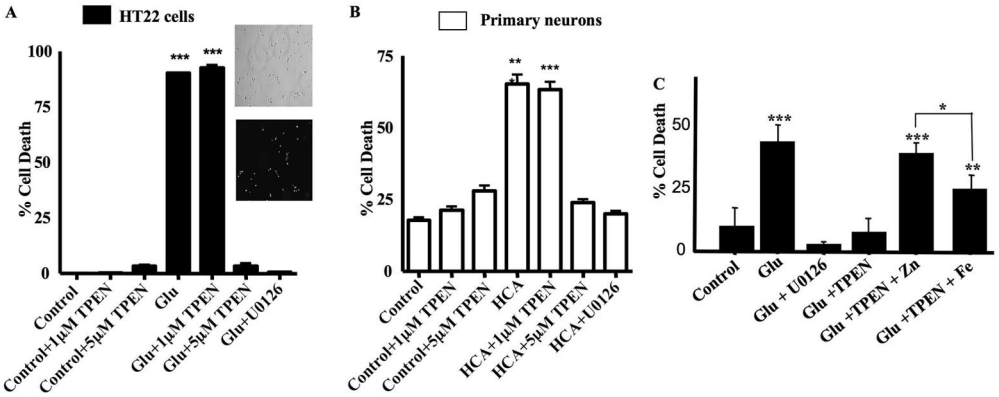

Fig. 7. TPEN blocks oxidative toxicity in HT22 cells and immature neurons. A, HT22 cells were treated with 1 μM TPEN, 5 μM TPEN, 5 mM glutamate, glutamate plus 1 μM TPEN, glutamate plus 5 μM TPEN, or glutamate plus 10 μM U0126. Toxicity was measured as the percentage of PI-positive cells after treatment for 12 h (mean ± S.E.M.; $n = 3$). ***, $p < 0.001$. TPEN (5 μM) blocks glutamate-induced oxidative toxicity in HT22 cells. Insets show typical results from a PI staining assay (with corresponding phase-contrast images) from control untreated (Con) and glutamate-treated (Glu) cells. B, immature neurons were treated with 1 μM TPEN, 5 μM TPEN, 5 mM HCA, HCA plus 1 μM TPEN, HCA plus 5 μM TPEN, or HCA plus 10 μM U0126. Toxicity was measured as the percentage of PI-positive cells after treatment for 16 h (mean ± S.E.M.; $n = 3$).***, $p < 0.001$. TPEN (5 μM) blocks HCA-induced oxidative toxicity in immature neurons. C, HT22 cells were treated with 5 mM glutamate or glutamate with the after additions: 10 μM U0126, 5 μM TPEN, 5 μM TPEN preincubated with 5 μM $ZnCl_2$, and 5 μM TPEN preincubated with 5 μM $FeCl_2$. Toxicity was measured as the percentage of PI-positive cells after treatment for 12 h (mean ± S.E.M.; $n = 4$). Toxicity was evaluated for statistical significance using one-way analysis of variance, with a Bonferroni multiple comparisons test. ***, $p < 0.001$ and **, $p < 0.01$ relative to control. *, $p < 0.05$, compared with toxicity between groups treated with glutamate and TPEN preincubated with $ZnCl_2$ versus those treated with glutamate and TPEN preincubated with $FeCl_2$.

that 5 μM TPEN was also required to block glutamate- and HCA-induced toxicity in HT22 cells and immature neurons, respectively, showing a close association between the inhibition of ERK1/2 activation, restoration of ERK1/2 phosphatase activity and protection from oxidative stress.

Because selective iron chelators block HCA-induced toxicity in immature neurons (Zaman et al., 1999) it is likely that TPEN exerts its protective effects via chelation of Fe^{2+} as well as Zn^{2+}. However, Fe^{2+} contributes *indirectly* to ERK1/2 phosphatase inhibition through its impact on ROS generation in HT22 cells and immature neurons unlike Zn^{2+}, which exerts a *direct* inhibitory effect on ERK1/2 phosphatases. Select phosphatase inhibition is also partially responsible for ERK1/2 activation in distinct brain regions vulnerable to a global ischemia insult (Ho et al., 2007). It remains to be established whether oxidative stress and/or intracellular free Zn^{2+} contributes to regional inhibition of ERK1/2 phosphatases in ischemic brain.

Previous results from our group suggest that PP2A is the major ERK1/2 phosphatase in immature neurons (Levinthal and Defranco, 2005) and HT22 cells (data not shown) but that other MAPK phosphatases in these cells contribute to the regulation of ERK1/2 activation. In a recent report, glutamate treatment of HT22 cells and immature neurons was found to trigger the degradation of MKP1 (Choi et al., 2006). Although MKP1 exerts a minor albeit significant effect on ERK1/2 activation and glutamate toxicity in HT22 cells (Choi et al., 2006), the loss of this enzyme cannot be solely responsible for heightened ERK1/2 activation because ERK1/2 phosphatase activity in extracts from oxidatively stressed neurons can be restored in vitro with DTT (Levinthal and Defranco, 2005). Furthermore, the JNK family of MAPKs is the preferred substrates of MKP1, which is inconsistent with the selective effects of oxidative stress in HT22 cells and immature neurons on ERK1/2 phosphatases. Because PP2A activity but not protein expression (i.e., of its C subunit) was reduced in glutamate-treated HT22 cells, oxidative stress in neurons can trigger both reversible (Levinthal and Defranco, 2005) and irreversible (Choi et al., 2006) alterations in distinct protein phosphatases that collectively could contribute to persistent activation of specific MAPKs.

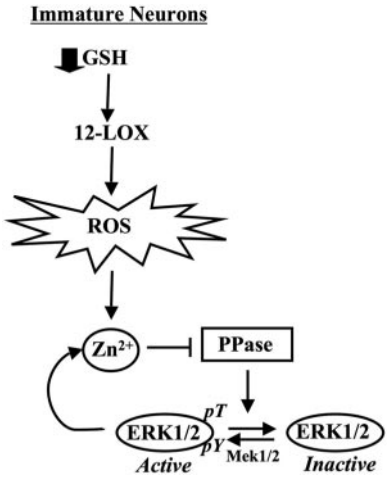

Fig. 8. Mechanism of ERK1/2-dependent neuronal cell death triggered by ROS-mediated Zn^{2+} accumulation. Accumulation of intracellular Zn^{2+} brought about by oxidative stress (ROS) in neurons inhibits protein phosphatases that act selectively on ERK1/2. ROS are generated in immature neurons after the depletion of glutathione (GSH) and subsequent activation of 12-lipoxygenase (12-LOX). The persistent activation of ERK1/2 (pERK1/2) functions to promote cell death in part through a positive feedback loop that maintains elevated Zn^{2+} levels.

The decreased accumulation of free Zn^{2+} upon inhibition of ERK1/2 activation by U0126 supports the existence of a positive feedback loop that not only provides conditions for the maintenance of ERK1/2 activation (i.e., through phosphatase inhibition) but also exacerbates neuronal cell exposure to neurotoxic levels of free Zn^{2+} (Fig. 7). In this case, ROS, which contribute to ERK1/2 activation in an 12-lipoxygenase-dependent manner (Stanciu et al., 2000; Fig. 8), provide the trigger that acts to promote the release of protein-bound Zn^{2+}, perhaps through thiol oxidation of specific cysteine residues that participate in Zn^{2+} binding (Aizenman et al., 2000). Thus, ERK1/2 may prevent the repair of oxidatively damaged Zn^{2+} binding proteins or limit their expression (Jiang et al., 2004). In the absence of oxidative damage to these proteins, long-term ERK1/2 activation may not affect intracellular Zn^{2+} homeostasis and promote cell death.

In summary, we have identified an important regulatory feature of protein phosphatase regulation, namely, reversible Zn^{2+} inhibition that triggers the persistent activation of a select MAPK signaling module in neurons. Furthermore, the oxidative induction of Zn^{2+} accumulation predisposes neuronal cells to a positive feedback loop driven by ERK1/2 that disrupts Zn^{2+} homeostasis and further exacerbates cellular exposure to neurotoxic levels of free Zn^{2+}.

Acknowledgments

We thank David Schubert (Salk Institute, San Diego, CA) for the kind gift of HT22 cells and David Giedroc (University of Indiana, Bloomington, IN) for the MRE-luciferase plasmid. We thank Dr. Karl Kandler for invaluable help and advice on the quantitative fluorescence measurement and for the use of equipment. We also thank Karen Hartnett for expert technical assistance.

References

Aizenman E, Stout AK, Hartnett KA, Dineley KE, McLaughlin B, and Reynolds IJ (2000) Induction of neuronal apoptosis by thiol oxidation: putative role of intracellular zinc release. *J Neurochem* **75:**1878–1888.

Alessandrini A, Namura S, Moskowitz MA, and Bonventre JV (1999) MEK1 protein kinase inhibition protects against damage resulting from focal cerebral ischemia. *Proc Natl Acad Sci U S A* **96:**12866–12869.

Choi BH, Hur EM, Lee JH, Jun DJ, and Kim KT (2006) Protein kinase Cdelta-mediated proteasomal degradation of MAP kinase phosphatase-1 contributes to glutamate-induced neuronal cell death. *J Cell Sci* **119:**1329–1340.

Cornell NW and Crivaro KE (1972) Stability constant for the zinc-dithiothreitol complex. *Anal Biochem* **47:**203–208.

Devinney MJ 2nd, Reynolds IJ, and Dineley KE (2005) Simultaneous detection of intracellular free calcium and zinc using fura-2FF and FluoZin-3. *Cell Calcium* **37:**225–232.

Farooq A and Zhou MM (2004) Structure and regulation of MAPK phosphatases. *Cell Signal* **16:**769–779.

Foley TD, Armstrong JJ, and Kupchak BR (2004) Identification and H_2O_2 sensitivity of the major constitutive MAPK phosphatase from rat brain. *Biochem Biophys Res Commun* **315:**568–574.

Frederickson CJ, Giblin LJ, Krezel A, McAdoo DJ, Mueller RN, Zeng Y, Balaji RV, Masalha R, Thompson RB, Fierke CA, et al. (2006) Concentrations of extracellular free zinc (pZn)e in the central nervous system during simple anesthetization, ischemia and reperfusion. *Exp Neurol* **198:**285–293.

Haase H and Maret W (2003) Intracellular zinc fluctuations modulate protein tyrosine phosphatase activity in insulin/insulin-like growth factor-1 signaling. *Exp Cell Res* **291:**289–298.

Hara H and Aizenman E (2004) A molecular technique for detecting the liberation of intracellular zinc in cultured neurons. *J Neurosci Methods* **137:**175–180.

Ho Y, Logue E, Callaway CW, and DeFranco DB (2007) Different mechanisms account for extracellular-signal regulated kinase activation in distinct brain regions following global ischemia and reperfusion. *Neuroscience* **145:**248–255.

Jiang H, Fu K, and Andrews GK (2004) Gene- and cell-type-specific effects of signal transduction cascades on metal-regulated gene transcription appear to be independent of changes in the phosphorylation of metal-response-element-binding transcription factor-1. *Biochem J* **382:**33–41.

Kamata H, Honda S, Maeda S, Chang L, Hirata H, and Karin M (2005) Reactive

oxygen species promote TNFalpha-induced death and sustained JNK activation by inhibiting MAP kinase phosphatases. *Cell* **120:**649–661.
Kim HJ, Chakravarti N, Oridate N, Choe C, Claret FX, and Lotan R (2006a) *N*-(4 Hydroxyphenyl)retinamide-induced apoptosis triggered by reactive oxygen species is mediated by activation of MAPKs in head and neck squamous carcinoma cells. *Oncogene* **25:**2785–2794.
Kim YM, Reed W, Wu W, Bromberg PA, Graves LM, and Samet JM. (2006b) Zn^{2+}-induced IL 8 expression involves AP-1, JNK, and ERK activities in human airway epithelial cells. *Am J Physiol Lung Cell Mol Physiol* **290:**L1028–L1035.
Knoch ME, Hartnett KA, Hara H, Kandler K, and Aizenman E (2008) Microglia induce neurotoxicity via intraneuronal Zn^{2+} release and a K^+ current surge. *Glia* **56:**89–96.
Koh JY and Choi DW (1994) Zinc toxicity on cultured cortical neurons: involvement of *N*-methyl-D-aspartate receptors. *Neuroscience* **60:**1049–1057.
Koh JY, Suh SW, Gwag BJ, He YY, Hsu CY, and Choi DW (1996) The role of zinc in selective neuronal death after transient global cerebral ischemia. *Science* **272:** 1013–1016.
Land PW and Aizenman E (2005) Zinc accumulation after target loss: an early event in retrograde degeneration of thalamic neurons. *Eur J Neurosci* **21:**647–657.
Levinthal DJ and Defranco DB (2005) Reversible oxidation of ERK-directed protein phosphatases drives oxidative toxicity in neurons. *J Biol Chem* **280:**5875–5883.
Li Y, Maher P, and Schubert D (1997) A role for 12-lipoxygenase in nerve cell death caused by glutathione depletion. *Neuron* **19:**453–463.
Luo Y and DeFranco DB (2006) Opposing roles for ERK1/2 in neuronal oxidative toxicity: distinct mechanisms of ERK1/2 action at early versus late phases of oxidative stress. *J Biol Chem* **281:**16436–16442.
Maret W, Jacob C, Vallee BL, and Fischer EH (1999) Inhibitory sites in enzymes: zinc removal and reactivation by thionein. *Proc Natl Acad Sci U S A* **96:**1936–1940.
McCulloch J and Dewar D (2001) A radical approach to stroke therapy. *Proc Natl Acad Sci U S A* **98:**10989–10991.
Meng TC, Fukada T, and Tonks NK (2002) Reversible oxidation and inactivation of protein tyrosine phosphatases in vivo. *Mol Cell* **9:**387–399.
Murphy TH, Schnaar RL, and Coyle JT (1990) Immature cortical neurons are uniquely sensitive to glutamate toxicity by inhibition of cystine uptake. *FASEB J* **4:**1624–1633.
Ryu H, Lee J, Zaman K, Kubilis J, Ferrante RJ, Ross BD, Neve R, and Ratan RR (2003) Sp1 and Sp3 are oxidative stress-inducible, antideath transcription factors in cortical neurons. *J Neurosci* **23:**3597–3606.
Satoh T, Nakatsuka D, Watanabe Y, Nagata I, Kikuchi H, and Namura S (2000) Neuroprotection by MAPK/ERK kinase inhibition with U0126 against oxidative stress in a mouse neuronal cell line and rat primary cultured cortical neurons. *Neurosci Lett* **288:**163–166.
Sensi SL and Jeng JM (2004) REthiniing the excitotoxic milieu: the emerging role of Zn^{2+} in ischemic neuronal injury. *Curr Mol Med* **4:**87–111.
Seo SR, Chong SA, Lee SI, Sung JY, Ahn YS, Chung KC, and Seo JT (2001) Zn^{2+}-induced ERK activation mediated by reactive oxygen species causes cell death in differentiated PC12 cells. *J Neurochem* **78:**600–610.
Stanciu M and DeFranco DB (2002) Prolonged nuclear retention of activated extracellular signal-regulated protein kinase promotes cell death generated by oxidative toxicity or proteasome inhibition in a neuronal cell line. *J Biol Chem* **277:** 4010–4017.
Tan S, Schubert D, and Maher P (2001) Oxytosis: a novel form of programmed cell death. *Curr Top Med Chem* **1:**497–506.
Thomas GM and Huganir RL (2004) MAPK cascade signalling and synaptic plasticity. *Nat Rev Neurosci* **5:**173–183.
Tonks NK (2003) PTP1B: from the sidelines to the front lines! *FEBS Lett* **546:**140–148, 2003.
Xia Z, Dickens M, Raingeaud J, Davis RJ, and Greenberg ME (1995) Opposing effects of ERK and JNK-p38 MAP kinases on apoptosis. *Science* **270:**1326–1331.
Yu JS (1998) Activation of protein phosphatase 2A by the Fe^{2+}/ascorbate system. *J Biochem* **124:**225–230.
Zaman K, Ryu H, Hall D, O'Donovan K, Lin KI, Miller MP, Marquis JC, Baraban JM, Semenza GL, and Ratan RR (1999) Protection from oxidative stress-induced apoptosis in cortical neuronal cultures by iron chelators is associated with enhanced DNA binding of hypoxia-inducible factor 1 and ATF-1/CREB and increased expression of glycolytic enzymes, p21(waf1/cip1), and erythropoietin. *J Neurosci* **19:**9821–9830.
Zhang Y, Wang H, Li J, Jimenez DA, Levitan ES, Aizenman E, and Rosenberg PA (2004) Peroxynitrite-induced neuronal apoptosis is mediated by intracellular zinc release and 12 lipoxygenase activation. *J Neurosci* **24:**10616–10627.
Zhuo S and Dixon JE (1997) Effects of sulfhydryl regents on the activity of lambda Ser/Thr phosphoprotein phosphatase and inhibition of the enzyme by zinc ion. *Protein Eng* **10:**1445–1452.

Address correspondence to: Dr. Donald B. DeFranco, Department of Pharmacology, University of Pittsburgh School of Medicine, 7041 BST 3, 3501 Fifth Ave., Pittsburgh, PA 15261. E-mail: dod1@pitt.edu